A&A 439, 521–526 (2005)
DOI: 10.1051/0004-6361:20053175

Astronomy & Astrophysics

The location of the broad H I absorption in 3C 305: clear evidence for a jet-accelerated neutral outflow⋆

R. Morganti[1], T. A. Oosterloo[1], C. N. Tadhunter[2], G. van Moorsel[3], and B. Emonts[4]

[1] Netherlands Foundation for Research in Astronomy, Postbus 2, 7990 AA, Dwingeloo, The Netherlands
e-mail: morganti@astron.nl
[2] Dep. Physics and Astronomy, University of Sheffield, Sheffield S7 3RH, UK
[3] National Radio Astronomy Observatory, Socorro, NM 87801, USA
[4] Kapteyn Astronomical Institute, University of Groningen, PO Box 800, 9700 AV Groningen, The Netherlands

Received 1 April 2005 / Accepted 3 May 2005

Abstract. We present high-spatial resolution 21-cm H I VLA observations of the radio galaxy 3C 305 ($z = 0.041$). These new high-resolution data show that the ~1000 km s^{-1} broad H I absorption, earlier detected in low-resolution WSRT observations, is occurring against the bright, eastern radio lobe, about 1.6 kpc from the nucleus. We use new optical spectra taken with the WHT to make a detailed comparison of the kinematics of the neutral hydrogen with that of the ionised gas. The striking similarity between the complex kinematics of the two gas phases suggests that both the ionised gas and the neutral gas are part of the same outflow. Earlier studies of the ionised gas had already found evidence for a strong interaction between the radio jet and the interstellar medium at the location of the eastern radio lobe. Our results show that the fast outflow produced by this interaction also contains a component of neutral atomic hydrogen. The most likely interpretation is that the radio jet ionises the ISM and accelerates it to the high outflow velocities observed. Our observations demonstrate that, following this strong jet-cloud interaction, not all gas clouds are destroyed and that part of the gas can cool and become neutral. The mass outflow rate measured in 3C 305 is comparable, although at the lower end of the distribution, to that found in Ultra-Luminous IR galaxies. This suggests that AGN-driven outflows, and in particular jet-driven outflows, can have a similar impact on the evolution of a galaxy as starburst-driven superwinds.

Key words. galaxies: active – galaxies: individual: 3C 305 – galaxies: ISM

1. Introduction

The immediate surroundings of active galactic nuclei (AGN) are complex regions characterised by extreme physical conditions. There, the interplay between the enormous amount of energy released from the nucleus and the ISM is most critical.

Gas outflows can be a result of such interaction. Fast nuclear outflows of *ionised* gas appear to be a relatively common phenomena in active galactic nuclei (see e.g. Crenshaw et al. 2003; Kriss et al. 2004; Capetti et al. 1999; Krongold et al. 2003; Veilleux et al. 2002; Tadhunter et al. 2001; Elvis 2000). They are mainly detected in optical, UV and X-ray observations. Gas outflows associated with AGN provide energy feedback into the interstellar medium (ISM) that can profoundly affect the evolution of the central engine as well as that of the host galaxy (e.g. Silk & Rees 1998; Rawlings & Jarvis 2004). The mass-loss rate from these outflows can be a substantial fraction of the accretion rate needed to power the AGN. Thus, they are an important element in the evolution of the host galaxy.

It is not too surprising that such outflows are also found in radio galaxies (see e.g. Tadhunter 1991; Tadhunter et al. 2001; Holt et al. 2003; van Bemmel et al. 2003; and Morganti et al. 2004, for a summary of recent results). However, it is intriguing that in several radio sources fast outflows of *neutral* hydrogen (up to 2000 km s^{-1}) have been discovered. The best examples so far are the radio galaxy 3C 293 (Morganti et al. 2003) and the radio-loud Seyfert galaxy IC 5063 (Oosterloo et al. 2000). The number of galaxies known to show broad H I absorption (ranging from 800 up to 2000 km s^{-1}) is, however, growing and therefore this appears to be a phenomenon that is relatively common and important in at least some radio sources (see Morganti et al. 2005, for a summary).

A number of mechanisms have been suggested to explain these outflows of neutral hydrogen. They range from starbust-driven superwinds (Heckman et al. 1990), adiabatically expanded broad emission line clouds (Elvis et al. 2002), dusty narrow-line regions that are radiation pressure dominated (Dopita et al. 2002), to outflows driven by the radio jet. Different characteristics, in particular the location where the outflow is occurring, can be expected depending on the origin. For example, if connected to the broad line regions, we

⋆ Based on observations with the Very Large Array.

expect to find the outflow located at (or very close to) the nucleus. If the outflows are driven by the radio jet, we expect an association between strong radio features and the location of the outflow. Such an association does not necessarily occur in the case of radiation driven outflows. So far, direct information about the location of the outflow is available only for one object (IC 5063) and through indirect arguments for a second case, 3C 293 (Emonts et al. 2005). The reason that this information is available only for such a small number of cases is that high resolution H I observations performed with a broad enough observing band as well as high sensitivity are difficult to obtain.

Here we present results from VLA observations designed to locate the broad H I absorption in the radio galaxy 3C 305. 3C 305 is a relatively compact radio galaxy (Heckman et al. 1992; Jackson et al. 2003) of only about 5 arcsec (about 4 kpc) in size. On this small scale, 3C 305 has a complex structure with two jets forming radio lobes separated by 3.6 arcsec in PA 54° as seen in MERLIN observations (Jackson et al. 2003) as well as two low-brightness arms extending perpendicular to the radio axis that have been detected with the VLA (Heckman et al. 1982). Deep and relatively narrow H I absorption was detected in the high-resolution observations done with MERLIN (Jackson et al. 2003). However, recent broad-band Westerbork Synthesis Radio Telescope (WSRT) observations have revealed that a broad H I absorption component is also present (Morganti et al. in prep.). The spectrum from these data is shown in Fig. 1. The MERLIN observations have a limited bandwidth and insufficient sensitivity to detect the broad H I absorption component while at the typical 21-cm WSRT resolution of ∼13 arcsec, 3C 305 appears spatially unresolved. Thus, deeper high-spatial resolution *and* broader-band observations are needed to locate the region where the broad H I absorption is occurring.

Throughout this paper we will assume $H_0 = 75\ \mathrm{km\,s^{-1}\,Mpc^{-1}}$. At the redshift of 3C 305 ($z = 0.041$) this implies a distance of 167 Mpc, hence 1 arcsec is equivalent to 810 pc.

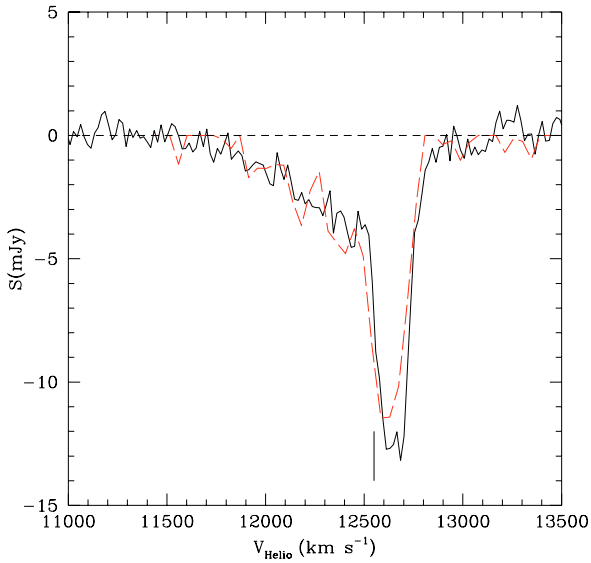

Fig. 1. H I absorption profile obtained with the WSRT with a velocity resolution of ∼17 $\mathrm{km\,s^{-1}}$ (solid line). The profile shows a deep, relatively narrow, absorption and a broad component that covers more than 1000 $\mathrm{km\,s^{-1}}$ at zero intensity. The systemic velocity is also indicated. The long-dashed profile shows the integrated spectrum from the VLA data (at lower velocity resolution, see text for details). The similarity of the two profiles indicates that basically all the absorbed flux is recovered from the high-resolution VLA observations.

2. High resolution observations of the H I absorption

2.1. VLA observations

The H I observations were obtained using the VLA in the A-array configuration on 23 Sep. 2004 with a total integration time on source of 3.8 h. The central frequency used was 1363.8 MHz. This frequency is offset compared to the frequency corresponding to the systemic velocity of the galaxy, but corresponds to *the central velocity of the entire* H I *absorption* detected by the WSRT. This was done in order to make sure that enough continuum would be available at both sides of the profile. The observations made use of the 12-MHz bandwidth and 64 channels. In order to use this configuration, we observed only one polarisation (1 IF). The velocity resolution obtained is relatively low, only ∼40 $\mathrm{km\,s^{-1}}$ (before Hanning smoothing), nevertheless good enough for the detection of the broad component. The need for (at least!) 12-MHz is clear from the width of the H I profile. The data reduction, including bandpass calibration and continuum subtraction, was done using both the AIPS and Miriad packages. A line cube was made using uniform and robust weighting (using robustness equal to zero). The results presented below, and the figures have been obtained for the robustness equal zero data. The beam size is 1.2×1.0 arcsec in PA $= -18.7°$. The noise per channel (after Hanning smoothing) is 0.29 mJy beam^{-1}.

From the line-free channels, a continuum image was made. This image is shown in Fig. 2 (rms noise 1.9 mJy beam^{-1}).

2.2. Results

In Fig. 2 the total intensity of the H I absorption is shown as a grey scale image with superimposed contours representing the continuum image. The H I absorption is spatially extended and is detected across the brighter part of the radio source. The most important result from these observations can be seen in the position-velocity plot of Fig. 2, obtained from a slice passing through the two lobes and the core. The deep and relatively narrow part of the H I absorption appears coincident with the SW radio lobe, as seen before in the MERLIN observations of Jackson et al. (2003). However, the broad H I absorption appears to be located in the region of the bright eastern radio lobe, about 1.6 kpc from the nucleus. This broad component was not seen in the observations of Jackson et al. who used a narrower band. The broad absorption is weak. Nevertheless, the comparison between the integrated H I profile from the VLA data with the WSRT profile shows a great similarity (Fig. 1) indicating that basically all the absorbed flux is recovered from the high-resolution observations.

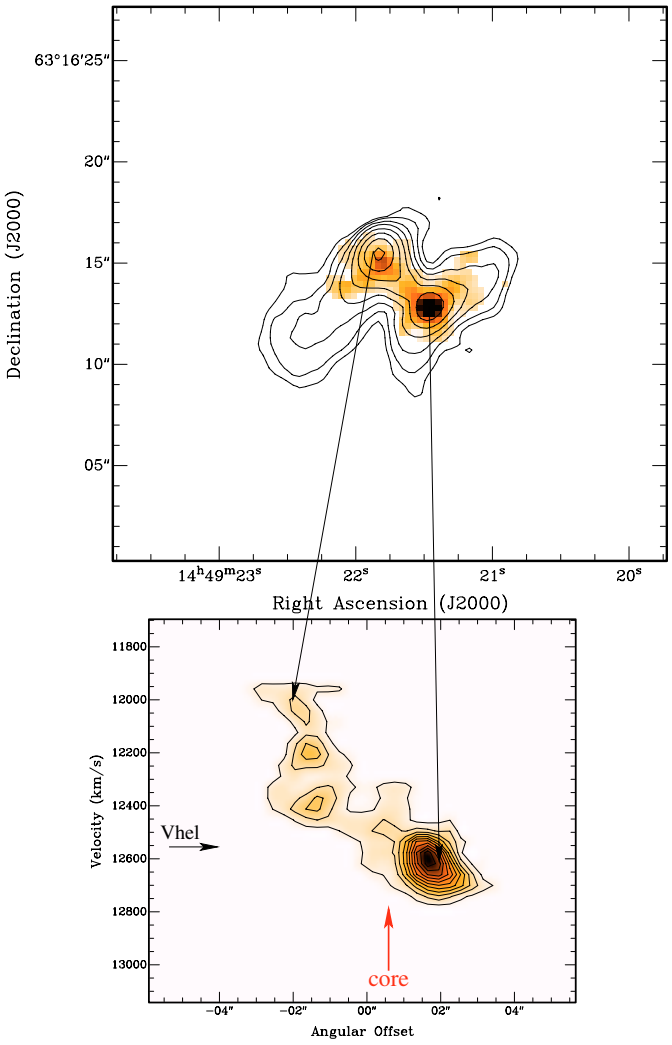

Fig. 2. Panel showing *(top)* the radio continuum image (contour) and the integrated H I absorption (grey scale). *(Bottom)* The position-velocity plot from a slice passing through the two lobes. The contour levels for the continuum image are 10 mJy beam^{-1} to 830 mJy beam^{-1} in steps of a factor 2. The grey scale image represents the total intensity of the H I absorption. The contour levels of the H I are −0.7, ..., –7.7 mJy beam^{-1} in steps of 0.7 mJy beam^{-1}. The arrow represents the systemic velocity.

The narrow, deep component that covers the SW lobe is spatially resolved and shows a velocity gradient across the lobe. The optical depth of this component is $\tau = 0.02$ corresponding to a column density of $N_{\rm H\,I} = 5.4 \times 10^{20}\ T_{\rm spin}/(100\ {\rm K})\ {\rm cm}^{-2}$. This component (centered on $V_{\rm hel} = 12627$ km s^{-1}) was interpreted by Jackson et al. (2003) as due to the nuclear dust lane being located in front of the SW radio lobe and the SW radio jet pointing away from us. The absence of a similar narrow component, in their data, against the NE lobe was interpreted as this lobe being in front of the dust lane and the NE jet pointing towards us. Our new observations show that the faint H I absorption is detected in the region going from the nucleus of 3C 305 up to the bright NE radio lobe. Some of this fainter absorption could be due to part of the dust-lane being in front of the central and some of the NE radio emission. The velocity gradient near the core could reflect the rotation of the dust-lane material about the centre of 3C 305. However, the overall H I absorption spans over such a wide range of velocities (more than 1000 km s^{-1}) that not all motions can be due to galactic rotation. In order to investigate this in more detail, we will below compare the velocities of the neutral hydrogen with those of the ionised gas (see Sect. 3).

The optical depth of the shallow H I absorption is only $\tau \sim 0.0023$ in the region of the peak of the NE radio lobe and increases along the eastern jet reaching $\tau \sim 0.01$ at the position of the nucleus. The column density of the broad component is $N_{\rm H\,I} \sim 2 \times 10^{21}\ T_{\rm spin}/(1000\ {\rm K})\ {\rm cm}^{-2}$. For this component we have assumed a $T_{\rm spin} = 1000$ K. The presence of a strong continuum source near the H I gas, as well as the fact that the gas has likely just passed through a strong shock, can make the radiative excitation of the H I hyperfine state to dominate over the, usually more important, collisional excitation (see e.g. Bahcall & Ekers 1969). Under these conditions, the spin temperature is, therefore, likely to be of the order of 1000 K or more. Using the above column density, the total H I mass of the outflowing gas can be estimated. The outflowing neutral hydrogen appears to cover the NE lobe, we therefore use a region of 1×1 kpc in size. The resulting mass is about $1.3 \times 10^7\ M_\odot$. The size of the region is an uncertain parameter in this calculation. However, one should also keep in mind that our observations cannot detect H I located behind of the radio continuum, therefore more neutral hydrogen could be in principle present in the region. Thus, the estimated value should give a realistic value to the H I mass involved in the outflow.

3. The ionised gas

In order to obtain more complete information about the kinematics of the gas, we have investigated the characteristics of the ionised gas using available long-slit spectra of 3C 305 obtained with the ISIS dual-beam spectrograph on the William Herschel Telescope (WHT) on La Palma. The wavelength range covers 3300 to 7300 Å (in the rest frame of 3C 305), the resolution is 3.6 Å (or ∼165 km s^{-1} in the red part of the spectrum) and the wavelength calibration has an accuracy of ∼1 Å (or 50 km s^{-1} at Hα). A more detailed description of the observations and data reduction is given in Tadhunter et al. (2005).

The presence of extended emission lines with complex kinematics was already known from the work of Heckman et al. (1982). The [O III] 5007 Å region of the new spectra (after the subtraction of the galaxy's continuum) obtained along PA 60° (the galaxy's major axis) and along PA 42° (the radio axis) are shown in Fig. 3. The location of the peaks of the radio lobes is marked. For comparison, in the bottom figure, the white contours give the data from the position-velocity slice (same as Fig. 2) of the H I obtained along the same (radio) axis. From both figures it is immediately clear how complex and kinematically disturbed the ionised gas is in the region exactly co-spatial with the bright radio emission, in particular on the eastern side.

The spectrum taken along the major axis of the galaxy (Fig. 3, (top)) shows – most clearly outside the region of the radio emission – the signature of the regularly rotating, large-scale disk of the galaxy, with amplitude of about 400 km s^{-1} (see also Heckman et al. 1982). The velocity at the location

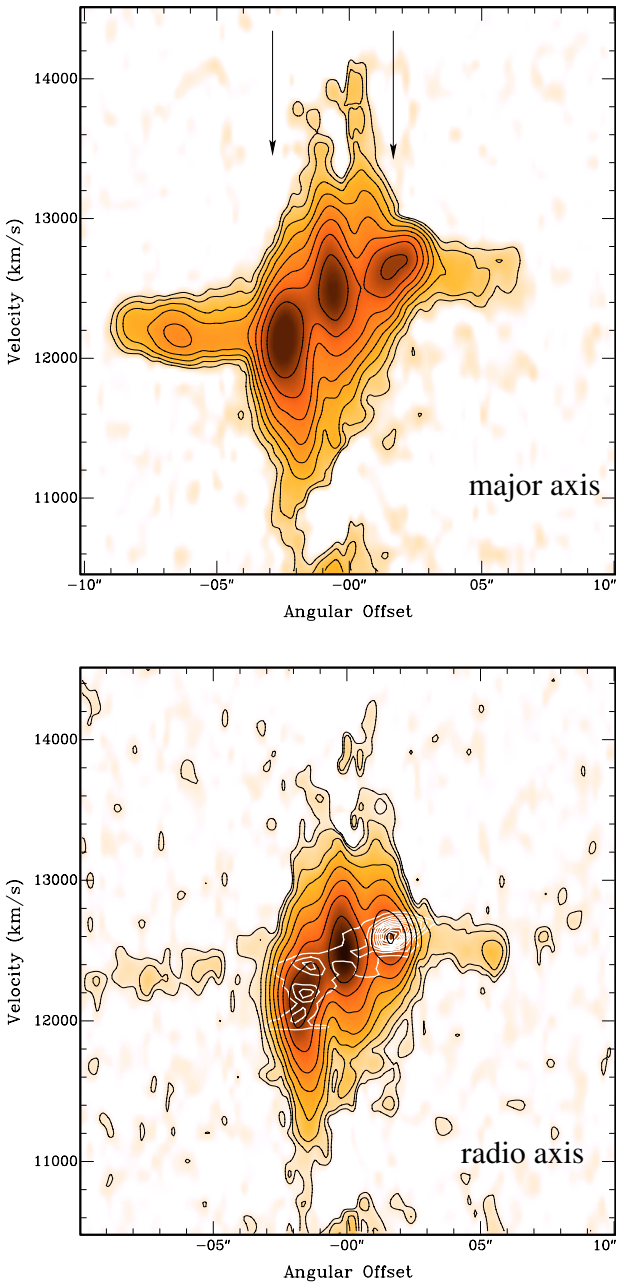

Fig. 3. *Top*: WHT spectrum of the [O III] region of 3C 305 (after the subtraction of the continuum from the galaxy) taken in PA 60°, i.e. along the galaxy's major axis (NE to the left, SW to the right). The two arrows represent the approximate position of the peak of the radio lobes. *Bottom*: WHT spectrum of the [O III] region of 3C 305 (black contours and greyscale) taken in PA 42°, i.e. along the radio axis. White contours represent the H I position-velocity plot taken along the radio axis (as in Fig. 2).

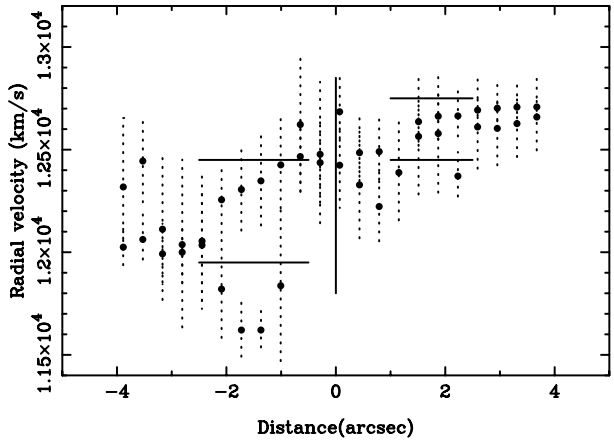

Fig. 4. Plot showing the centroid and *FWHM* of double Gaussian fits to the Hα line from the spectrum taken along the radio axis (PA 42°, NE to the left, SW to the right). The dashed lines represent the range of velocities encompassed by the *FWHM* of each Gaussian component (corrected for instrumental broadening). The horizontal lines represent the spatial and velocity ranges covered by the H I absorption. The vertical solid line represents the full range of radial velocity covered by the WSRT H I profile.

of the peak of the optical continuum emission, that we associate with the nucleus, is 12 550 km s^{-1}, consistent with the previous measurements of the systemic velocity of this galaxy (Heckman et al. 1982). In addition to the rotation, on the eastern side the ionised gas has a broad and asymmetric (mostly blueshifted) component, while on the western side broad redshifted emission is detected. Given the orientation of the radio source (as discussed in Sect. 2.2), this pattern is indicates a radial outflow of the ionised gas.

In Fig. 3 (bottom) the spectrum obtained along the radio axis (PA 42°) is shown, together with the H I position-velocity data. This allows a more consistent comparison between the kinematics of the neutral hydrogen and the ionized gas. Along this position angle, the quiescent, rotating gas is still visible although with a smaller amplitude because the slit is not along the major axis. Also in this position angle, a broad and blueshifted component of the ionised gas is observed NE of the core, while in the SW the profiles have a, somewhat narrower, redshifted wing.

The overlay of the H I position-velocity plot makes clear that the neutral hydrogen seen in absorption is formed by two components. Some of the H I belongs to the rotating dust-lane structure. As mentioned above, this is the case for the gas seen against the SW radio lobe and part of this structure could extend at least to the position of the nucleus and slightly beyond. Near the NE lobe, the H I profile clearly deviates by almost 500 km s^{-1} (FWZI) from the kinematics of the quiescent gas in the galaxy disk – in a similar way as the broad, blueshifted component of [O III].

The interesting result from the comparison in Fig. 3 is therefore that the broad, blueshifted H I is found at the location of maximum disturbance of the ionized gas on the eastern side region. This strongly suggests that *the two components of the gas are the result of a gaseous outflow produced by the same mechanism.*

The kinematics of the ionized gas are illustrated in more detail in Fig. 4 where the centroid and *FWHM* of double Gaussian fits to the Hα line along the radio axis (PA 42°) are shown. At all locations two Gaussians are required to provide an adequate fit to each of the lines in the Hα+[N II] blend, but it is clear from the plot that the splitting between the two

Gaussian components is particularly extreme at radial distances between 1 and 2 arcseconds NE of the nucleus. This is, therefore, between the nucleus and the peak intensity of the NE radio lobe. In the region coincident with the radio lobe there is no evidence for line splitting in Hα but two Gaussians are required to fit the lines, and the broader of the two components ($FWHM \sim 700$–$800\,\mathrm{km\,s^{-1}}$) is broader than can be explained by gravitational motions in a quiescent disk. Note that the velocity range encompassed by the *FWHM* of the optical emission lines in the region of line splitting 0.6 and 1.2 arcsec to the NE of the nucleus ($\Delta V \sim 1100\,\mathrm{km\,s^{-1}}$) is significantly larger than the range covered by the H I absorption at the same location ($\Delta V \sim 500\,\mathrm{km\,s^{-1}}$), although the direction of the kinematic disturbance (blueshift relative to quiescent disk) is the same for both components.

The mass of the ionized gas is directly related to the Hβ luminosity and the density of the gas can be estimated using standard formula (Osterbrock 1989). We have estimated this mass in the region of the eastern lobe. The *total* Hβ luminosity in this region is $1.16 \times 10^{40}\,\mathrm{erg\,s^{-1}}$. The measured value of the Hα/H$_\beta$ ratio (~3.6) is close to the case B recombination value, suggesting that the Hβ luminosity is relatively unaffected by dust extinction in this region. From the ratio of the [S II]λ6716/[S II]λ6731 lines we derive an upper limit to the density of 500 $\mathrm{cm^{-2}}$. Using these numbers we derive a lower limit to the mass of the ionized gas in the region of the eastern radio lobe of $2\times10^5\,M_\odot$. Therefore, unless the actual density is two orders of magnitude less than our upper limit – improbable given that the gas is likely to have been compressed in a fast, radiative shock – this shows that the mass of gas in the ionized outflow is much less than that in the neutral outflow.

4. An off-nuclear gas outflow

The high-resolution *and* the broad-band of new H I observations of the radio galaxy 3C 305 have allowed us to establish that the blueshifted H I component in this galaxy is located in the region of the NE bright radio lobe. Compared with the velocities of the quiescent gas in the galaxy disk, this neutral hydrogen is blueshifted by up to 500 $\mathrm{km\,s^{-1}}$. This is an important result as it confirms that neutral hydrogen with very disturbed kinematics is observed at kpc distances from the nucleus. In the case of 3C 305 the most blueshifted component of the H I absorption is located at 1.6 kpc from the nucleus.

While the presence of broad H I absorption is known now for a growing number of radio sources (Morganti et al. 2005), the information about the location of such absorption is still lacking in most of the cases. The only exception is the radio loud Seyfert galaxy IC 5063 (Oosterloo et al. 2000) and, through indirect arguments that will need to be confirmed by high-spatial resolution radio data, in the radio galaxy 3C 293 (Emonts et al. 2005). For these two cases we have argued that the most likely mechanism to produce the observed outflows of both ionised and neutral hydrogen is the interaction between the radio jets and the surrounding (dense) ISM. In the case of 3C 305 the evidence is also clearly in favour of this explanation.

Evidence of the presence of a strong interaction between the radio plasma and the surrounding interstellar medium was already obtained in the case of 3C 305 from previous optical studies. For example, a dense environment has been suggested to be the cause of the "H" shaped radio morphology. It has been argued, based on the highly disturbed kinematics and outflowing ionised gas (Heckman et al. 1982) as well as the coincidence of [Fe II] emission with the knot at the end of the NE radio jet (Jackson et al. 2003), that the interaction is particularly strong on the NE side. The broad, blueshifted H I is found at the location of maximum disturbance of the ionized gas. This, therefore, confirms that *fast outflows of neutral hydrogen can be produced by the interaction between the radio jet and the surrounding dense medium*. The presence of neutral gas in this region indicates that the gas can cool very efficiently following a strong jet-cloud interaction. Furthermore, it shows that the clouds are not destroyed by this interaction. This is in agreement with the results obtained by the numerical simulations used to investigate cases of jet-induced star formation by Mellema et al. (2002) and Fragile et al. (2004).

Interestingly, the comparison of the velocities shows that the the broad, blueshifted H I absorption does not encompass the the full range of blueshifted velocities covered by the ionized gas. To begin with, one should bear in mind that the blueshifted H I is very faint and we may be limited by sensitivity in detecting very broad H I absorption at every location (i.e. even if broader components are present we do not have the sensitivity of detecting them at locations where the continuum is not as strong as at the peak of the NE lobe). Nevertheless, there may be some physical reasons for the difference. The numerical simulations of clouds in radio galaxy cocoons overtaken by a strong shock wave (Mellema et al. 2002) show that in that scenario the cooling times for the dense fragments can be very short (only a few times 10^2 years). However, the gas accelerated to the highest velocities is of low density and may not have had time to cool. Alternatively, the higher-velocity clouds may be destroyed before they cool.

Another consideration is the geometry of the jet-cloud interaction. This may, for example, explain why the highest velocities of the ionized gas are observed in the region between the nucleus and the NE radio hot-spot. If the acceleration of the gas is due to a bowshock at the location of the hotspot, most of the acceleration of the gas at that location may happen in the direction perpendicular to the line of sight. On the other hand, further back along the jet the observed velocities of the gas are due to the lateral expansion of the lobe (mainly along the line of sight). Moreover, only the neutral hydrogen located in front of the radio source can be detected, while this is not the case for the ionized gas. Hence, the full kinematics of the H I may not be observable.

The mass outflow rate of the neutral hydrogen is significant. We can adopt the simple model used in Heckman (2002) and Rupke et al. (2002) to estimate a mass outflow rate. Following Heckman (2002)

$$\dot{M} = 30 \cdot \frac{\Omega}{4\pi} \cdot \frac{r_*}{1\,\mathrm{kpc}} \cdot \frac{N_\mathrm{H}}{10^{21}\,\mathrm{cm^{-2}}} \cdot \frac{v}{300\,\mathrm{kms^{-1}}}\, M_\odot\,\mathrm{yr^{-1}} \qquad (1)$$

where the mass is flowing into a solid angle Ω at a velocity v from a radius r_*. Using the column density derived above ($N_{\mathrm{H\,I}} \sim 2 \times 10^{21}$ $\mathrm{cm^{-2}}$) and a mean velocity of the outflow

between 200 and 300 km s^{-1}, we obtain a mass outflow rate of between 20 and 30 $M_\odot$ yr^{-1} for the neutral gas if we assume that the outflow covers 2π steradians on the sky, and between 5 and 7.5 $M_\odot$ yr^{-1} if we assume that the outflow covers only $\pi/2$ steradians.

Thus, the derived outflow rates are higher than those estimated for the ionised gas (from UV and X-ray observations) in nearby AGN (Crenshaw et al. 2003). The outflow rate measured in 3C 305 is, instead, comparable, although at the lower end of the distribution, to that found in Ultra Luminous IR galaxies by Rupke et al. (2002). The outflows observed in those galaxies are related to starburst-induced superwinds (Heckman et al. 1990) and they have been considered to have a major impact on the evolution of galaxies because of the feedback effects that these outflows can have (see e.g. Veilleux et al. 2002; Heckman 2002). Thus, our result shows that AGN-driven outflows and in particular jet-driven outflows, can have a similar amplitude and, therefore, can also have a similar impact on the evolution of galaxies. This supports the results from numerical simulations (Di Matteo et al. 2005) in which the energy released by the AGN can quench both star formation and the further growth of the black hole, thus explaining the relationship between the black hole mass and other properties of the galaxy. In the case of 3C 305, a significant burst of star formation took place between 0.4 and 1.5 Gyr ago (Tadhunter et al. 2005). Despite this stellar burst, the medium surrounding the radio source is still very dense and only the radio jet seems to be able to clear this gas.

Finally, the H I outflow in 3C 305 may have interesting connections with the detection of strong and blueshifted H I absorbers (column density 10^{18}–$10^{19.5}$ cm^{-2}) in the Lyα profiles of high redshift radio galaxies (see e.g. Wilman et al. 2004 and ref. therein). A possible way to explain this is via a highly supersonic jet expanding into the dense medium of a young radio galaxy that then consequently will be surrounded by an advancing quasi-spherical bow shock, as investigated via numerical simulation by Krause (2002). The study of the stellar population in 3C 305 suggests that this galaxy went through a gas-rich, major merger in its recent past. This radio galaxy may, therefore, represent an ideal example of nearby object having characteristics very similar to those of typical high redshift radio galaxies.

Acknowledgements. The National Radio Astronomy Observatory is a facility of the National Science Foundation operated under cooperative agreement by Associated Universities, Inc.

References

van Bemmel, I. M., Vernet, J., Fosbury, R. A. E., & Lamers H. J. G. L. M. 2003, MNRAS, 345, L13
Capetti, A., Axon, D. J., Macchetto, F. D., et al. 1999, ApJ, 516, 187
Crenshaw, D. M., Kraemer, S. B., & George, I. M. 2003, ARA&A, 41, 117
Di Matteo, T., Springel, V., & Hernquist, L. 2005, Nature, in press [arXiv:astro-ph/0502199]
Dopita, M. A., Groves, B. A., Sutherland, R. S., et al. 2002, ApJ, 572, 753
Elvis, M. 2000, ApJ, 545, 63
Elvis, M., Marengo, M., & Karovska, M. 2002, ApJ, 567, L107
Emonts, B. H. C., Morganti, R., Tadhunter, C. N., et al. 2005, MNRAS, submitted
Fragile, P. C., Murray, S., Anninos, P., & van Breugel, W. 2004, ApJ, 604, 74
Heckman, T. M. 2002, in Extragalactic Gas at Low Redshift, ed. J. Mulchaey, & J. Stocke, ASP Conf. Ser., 254, 292 [arXiv:astro-ph/0107438]
Heckman, T. M., Miley, G. K., Balick, B., van Breugel, W., & Butcher, H. R. 1982, ApJ, 262, 529
Heckman, T. M., Armus, L., & Miley, G. 1990, ApJS, 74, 833
Holt, J., Tadhunter, C., & Morganti, R. 2003 MNRAS, 342, 227
Jackson, N., Beswick, R., Pedlar, A., et al. 2002, A&A, 395, L13
Krause, M. 2002, A&A, 386, L1
Kriss, G. 2004, in The Interplay among Black Holes, Stars and ISM in Galactic Nuclei, ed. Storchi-Bergmann et al., IAU Symp. 222, in press [arXiv:astro-ph/0403685]
Krongold, Y., Nicastro, F., Brickhouse, N. S., et al. 2003, ApJ, 597, 832
Morganti, R., Oosterloo, T. A., Emonts, B. H. C., van der Hulst, J. M., & Tadhunter, C. 2003, ApJ, 593, L69
Morganti, R., Oosterloo, T., Emonts, B. H. C., Tadhunter, C. N., & Holt, J. 2004, Proc. IAU Symp., Recycling Intergalactic and Interstellar Matter, ed. P.-A. Duc, J. Braine, & E. Brinks, ASP, 217, 332 [arXiv:astro-ph/0310629]
Morganti, R., Oosterloo, T. A., & Tadhunter, C. N. 2005, in Extraplanar Gas, ed. R. Braun, ASP Conf., 331, in press [arXiv:astro-ph/0410222]
Oosterloo, T. A., Morganti, R., Tzioumis, A., et al. 2000, AJ, 119, 2085
Osterbrock, D. E. 1989, The Astrophysics of Gaseous Nebulae and Active Galactic Nuclei (Mill Valley, CA: University Science Books)
Rawlings, S., & Jarvis, M. J. 2004, MNRAS, in press [arXiv:astro-ph/0409687]
Rupke, D. S., Veilleux, S., & Sanders, D. B. 2002, ApJ, 570, 588
Tadhunter, C. 1991, MNRAS, 251, 46
Tadhunter, C., Wills, K., Morganti, R., Oosterloo, T., & Dickson, R. 2001, MNRAS, 327, 227
Tadhunter, C., Robinson, T. G., González Delgano, R. M., Wills, K., & Morganti, R. 2005, MNRAS, 356, 480
Veilleux, S., Cecil, G., Bland-Hawthorn, J., & Shopbell, P. L. 2002, RMxAC, 13, 222
Silk, J., & Rees, M. J. 1998, A&A, 331, L1
Wilman, R. J., Jarvis, M. J., Röttgering, H. J. A., & Binette, L. 2004, MNRAS, 351, 1109